Assessment of the amplitude of variations in total solar irradiance in the past.

© 2025 M.G. Ogurtdov[a,b,*]

[a]*Ioffe institute, St. Petersburg, Russia,*

[b]*Central Astronomical Observatory of the Russian Academy of Sciences at Pulkovo, St. Petersburg, Russia.*

******e-mail:maxim.ogurtsov@mail.ioffe.ru*

Received April 16, 2024
Revised August 29, 2024
Accepted September 26, 2024

An assessment was made of how reliably various modern reconstructions of total solar irradiance reconstruct long-term changes in this value in the past. To solve this problem, a forecast of long-term changes in total solar radiation in 1978−2017 was made using seven reconstructions covering the last 12−13 centuries. The paleoreconstructions used describe long-term variations with average amplitudes from 0.22 W m-2 (series with low amplitude) to 2.36 W m^{-2} (series with high amplitude). A nonlinear analog prediction method was applied, and the prediction results were compared with the actually measured values. It turned out that the experimentally measured variations in total solar radiation are better predicted by the low-amplitude reconstructions. However, the possibility that solar radiation in the past experienced more significant variations and the increase in total solar radiation after the Maunder Minimum reached 2.5 W m^{-2} cannot be completely excluded yet. Possible climatic consequences of such solar radiation variations are discussed.

DOI: 10.31857/S00167940250212e7

1. INTRODUCTION

Total solar irradiance (TSI) is the value of the integral over the entire spectrum of solar energy flux arriving at the upper part of the Earth atmosphere at the average distance between the Sun and the Earth. Variations in this value are closely related to changes in the magnetic activity of the Sun. Therefore, information on the temporal variations of TSI is of considerable interest for solar astrophysics. However, at present this information is very limited. What is the amplitude of long-term variations of this quantity? Does TSI always change synchronously with the main solar cycles? Are TSI variations completely determined by corresponding changes in the number of sunspots and

faculae? The answers to these questions are not entirely clear, primarily due to the brevity of experimental data on total solar radiation - systematic and reliable instrumental measurements of TSI began only in 1978.

In addition to purely scientific interest, data on TSI variations have practical significance, as radiation coming from the Sun is one of the climate-forming factors. Climate has a strong influence on many aspects of social and economic activities of humanity, which is why the well-known problem of global warming (GW) has already moved from the realm of purely scientific interests to the global political agenda. However, the physical mechanisms behind GW contain uncertainties, and their discussion continues. The lack of knowledge about long-term TSI variations creates one of these uncertainties. To date, using methods of solar paleoastrophysics, a number of TSI reconstructions have been obtained, covering time periods significantly longer than the last 40 years. However, these paleoreconstructions differ significantly and demonstrate a large difference in the amplitudes of secular variations [Solanki et al., 2013; Kopp, 2016; Chatzistergos et al., 2023]. These reconstructions can be divided into two classes: series with low amplitude of long-term changes (LA-series) and series with high amplitude of similar fluctuations (HA-series) [Connolly et al., 2021]. In recent IPCC reports, the prevailing opinion is that GW is mainly the result of increasing greenhouse gas concentrations and other types of anthropogenic activities, while the contribution of other natural phenomena, including solar activity, is insignificant (see [IPCC 2014, 2021]). For example, the AR5 report [IPCC, 2014] effectively only considers LA reconstructions and states that radiative forcing caused by TSI changes over the period 1750-2011 is 0.05 W m^{-2} with medium confidence. The AR6 report [IPCC, 2021] adopts a wider range of estimates of TSI changes over the past few centuries and concludes that TSI between the Maunder Minimum (1645-1715) and the second half of the 20th century may have increased by 0.7-2.7 W m^{-2}. The latest IPCC report [Gulev et al., 2021] mentions one of the HA reconstructions [Egorova et al., 2018] among the latest achievements, but preference is still given to LA-type reconstructions [Lean, 2000; Matthes et al., 2017; Jungclaus et al., 2017]. This suggests a minor contribution of solar activity to long-term climate changes. Obviously, the question of what was the real amplitude of TSI variations in the past is important not only for solar astrophysics but also for modern climatology. Answering this question is not easy, as we do not know how accurately TSI paleoreconstructions describe the real changes of this value in the distant past. The main disadvantage of all TSI reconstructions is that their quality can hardly be assessed by direct comparison with observational results. First, some reconstructions end in 1978-2000 and cannot be compared with a significant part of the experimentally measured series. Second, when normalizing TSI reconstructions to instrumentally

measured values, authors are usually able to fit the reconstructed values quite well to the experimental ones for any type of reconstruction – see, for example, LA series in Fig. 2 from [Dewitte et al., 2022] and HA (top panel of Fig. 1 from [Shapiro et al., 2011]. Therefore, the accuracy of the match between the obtained reconstruction and the actually measured TSI value can hardly serve as a convincing criterion of its reliability.

This work is devoted to determining which type of TSI reconstructions - MA or BA series - better describes its variations in the past. To solve this problem, the following algorithm was applied: (*a*) forecasts of TSI changes in 1978-2017 were made using various types of solar radiation reconstructions as an information bank, see Ogurtsov [2009]; (*b*) the forecast results were compared with real, instrumentally measured TSI values; (*c*) an assessment was made of which type of reconstructions more accurately and reliably predicts real TSI changes.

It should be noted that today there are different versions of instrumentally measured TSI, based on different interpretations of satellite observations. Two experimental series, PMOD and ACRIM, demonstrate different long-term trends. The PMOD series shows a continuous downward trend in TSI throughout the entire measurement interval. The ACRIM series reveals an increase in TSI between the minimums of 1986 and 1996. In this work, the most modern generalized, or composite, TSI series (TSI composites) obtained in the following works were used.

1. Dudok de Wit et al. [2017], whose authors performed statistical weighting of all available measurement data using their individual uncertainties. This series covers the period 1978-2015 and has two versions: the first version is based on the original TSI data, and the second includes some instrumental corrections (https://www.issibern.ch/teams/solar radiation/TSI_composite_DeWit.txt).

2. Montillet et al. [2022], whose authors obtained a composite series by applying a three-step combination method to PMOD data (ftp://ftp.pmodwrc.ch/pub/data/irradiance/virgo/TSI/TSIcomposite/MergedPMOD_NobaselineScaleCycle23_JPM_April2023.txt). In this work, the CPMDF1 version of this series was used, covering 1980-2023.

In this work, three series of TSI data were used. A forecast of long-term changes in instrumentally measured values of this quantity was made using reconstructions of TSI of various types (SA and LA) covering the last 970-1130 years as a source (bank) of information. The aim of the work was to determine which types of reconstructions better predict long-term changes in the real TSI. Within the framework of the algorithm used, all reconstructions (both SA and LA) were considered equally reliable and accurate sources of information. A check was made of how well this assumption corresponds to reality.

2. DATA AND METHODS

Seven TSI reconstructions were used in the work – time series obtained in the works of Bard et al. [2000], Delaygue and Bard [2011], Shapiro et al. [2011], Steinhilber et al. [2012], Roth and Joos [2013], Wu et al. [2018], Egorova et al. [2018]. All these time series were obtained using data on the concentration of cosmogenic isotopes in terrestrial archives and cover time intervals of 12 centuries or more. TSI reconstructions based on sunspot number data were not used in this work because they are significantly shorter (no more than 4 centuries) and therefore less suitable for predicting long-term TSI changes. The time series used in the work are described in Table 1. Table 1 shows the standard deviations (STD) of these series and the increase in reconstructed TSI since the end of the 17th century, i.e., starting from the deepest part of the Maunder Minimum. The standard deviation was considered as a characteristic of the amplitude of long-term fluctuations ΔTSI and served as the basis for dividing reconstructions into SA and LA series. Reconstructions with STDI<1.0 W m $^{-2}$ were considered the SA series, and records with STD>10 W m $^{-2}$ were considered the LA series. The time series of Wu et al. [2018], Shapiro et al. [2011] were scanned and digitized electronically.

TABLE 1.

Three annually averaged composite TSI series – the corrected and uncorrected series TSID $_C$ and TSID $_U$, obtained in the work of Dudok de Wit et al. [2017], and the corrected series TSI $_{PMOD}$, obtained in the work of Montillet et al. [2022], are shown in Fig. 1.

FIG. 1.

Figure 1 *a* shows the annual mean values, and Figure 1 *b* shows the ten-year average values (averages for 1978-1987 (1980-1987 for TSI $_{PMOD}$), 1988-1997, 1997-2007, 2008-2017 (2008-2015 for TSID)). The uncertainties of the ten-year averaged TSI values were estimated through a statistical experiment using the TSI uncertainties provided by the authors for each day of measurements. Several thousand Monte Carlo simulations were performed, in each of which a surrogate series was constructed by adding a random value to each point of the experimental TSI series over the entire measurement interval. The random value was generated by Gaussian white noise with a standard deviation equal to the corresponding uncertainty value of the TSI series (these values were provided by the experimenters themselves). Thus, both the mean value and the standard deviation (uncertainty) of the TSI averaged over a decade were estimated. For all three composite series at all four points, the uncertainty was less than 0.01 W m $^{-2}$.

As can be seen from Figure 1 *b* , the long-term trend in the $TSID_U$ and $TSID_C$ series has a maximum in 2003 and is described by the sequence of values: TSI(1983)<TSI(1993)<TSI(2003)>TSI(2013). The TSI_{PMOD} series has a declining trend throughout the entire interval: TSI(1983)>TSI(1993)>TSI(2003)>TSI(2013). All TSI reconstructions used for predicting $TSID_U$ and $TSID_C$ were truncated in 1978 and normalized so that their value in that year coincided with the mean value of the 10-year averaged $TSID_U$ and $TSID_C$ series (1361.25 W m^{-2} in 1978 in both cases). All TSI reconstructions used for predicting TSI_{PMOD} were truncated in 1980 and normalized so that their value in that year coincided with the mean value of the 10-year averaged TSI_{PMOD} series (1361.42 W m^{-2} in 1980).

The study used data from Bard et al. [2000] starting from 844 and data from other authors starting from 700. The series from the work of Bard et al. [2000] was extrapolated to 1982 using TSI regression on the concentration of ^{10}Be . All data used, both instrumental and reconstructions for subsequent analysis, were homogenized as follows: (*a*) first, they were interpolated annually and, if necessary, smoothed over 11 years; (*b*) then, the series obtained in the previous step were interpolated by decades. The data series transformed in this way to a uniform format are shown in Fig. 2 . The resulting TSI reconstructions, consisting of 115-129 points with a step of 10 years, and instrumental series, consisting of four points (1983, 1993, 2003, 2013), were used in the subsequent analysis.

FIG. 2.

Nonlinear predictions were made using the analog method proposed in the work of Farmer and Sidorowich [1987], and then developed and generalized in the work of Sugihara and May [1990]. This method is based on reconstructing the trajectory of the dynamic system of the predicted series in pseudo-phase space. It is non-parametric, i.e., it takes into account only the information contained in the analyzed series itself and does not use any a priori information about the model that generated it. Testing this method on a number of signals, including chaotic series, correlated noises, and natural signals, has shown that it is capable of predicting them quite satisfactorily [Sugihara and May, 1990; Sugihara, 1994; Ogurtsov, 2009, 2022; Sarp et al., 2018]. The assessment of the predictive potential of TSI reconstructions and the predictive ability of the nonlinear forecasting methodology used was carried out by predicting 35 points of each series using the previous 80-94 points as an information bank. All predictions were made using attractor dimension d =3 and seven nearest neighbors. The dependence of the correlation coefficient between the predicted and actual values on the prediction time T_p (number of time steps T_p into the future) for some TSI reconstructions is shown in Fig. 3 *a* along with prediction errors (Fig. 3 *b*).

FIG. 3.

To assess the real prediction error made using TSI paleoreconstructions, the uncertainties of these time series should be taken into account. These uncertainties were estimated using data provided by the authors: ca 0.25 Wm $^{-2}$ for the series Delaygue and Bard [2011], ca 0.12 Wm $^{-2}$ for the series Roth and Joos [2013]; ca 0.1 Wm $^{-2}$ for the series Wu et al. [2018], 0.38−0.53 Wm $^{-2}$ for the series Steinhiliber et al. [2011], 0.1−0.5 Wm $^{-2}$ for the series Bard et al. [2000], 1.0 Wm $^{-2}$ for the series Egorova et al. [2018] and Shapiro et al. [2011]. Taking these uncertainties into account, the prediction error was estimated using the statistical experiment described in Ogurtsov [2022].

3. RESULTS AND DISCUSSION

The average decadal values of TSID $_C$ over the interval 1978−2015 (four points) are shown in Fig. 4 along with forecasts made using seven paleoreconstructions. All predictions were made using attractor dimension d =3 and seven nearest neighbors. In practice, this means that to predict a specific value Y_{n+1} (a) − a segment of three previous points was taken [Y_{n-2}, Y_{n-1}, Y_n], (b) − in the past, seven segments most similar to it were selected, of the type [Y_{n-m-2}, Y_{n-m-1}, Y_{n-m}], (c)− for each segment, the value Y_{n-m+1} was determined, (d) − all seven such predictions were averaged. For each forecast obtained in this way, the prediction error was estimated as the root mean square error – standard deviation between predicted and actually observed values:

$$STD_{pred}^{obs} = \sqrt{\frac{1}{N-1}\sum_{i=1}^{N}\left(TSI_i^{obs} - TSI_i^{pred}\right)^2}\ , (1)$$

where N =4. The attractor dimension (segment length) and the number of nearest neighbors were selected to minimize the value STD_{pred}^{obs} . Then the probability that the predicted series actually describes the observed changes in TSI was estimated using a statistical experiment. A series of Monte Carlo simulations was performed, in each of which a surrogate series was constructed by adding a random value to each of the four points of the predicted series (1983–2013). Each random value was generated using Gaussian white noise with a standard deviation equal to the corresponding prediction error value.

FIG. 4.

Then the value P - the probability that these surrogate series actually describe the experimental record, was estimated in two ways:

(a) the value P_1 - the probability that the average value of the predicted series during 1978-2015 or 1980-2023 would have a deviation from the average value of the real experimental series by no more than 1.0 W m $^{-2}$;

(*b*) a second condition was added to the first one - in addition to the average deviation of less than 1.0 W m $^{-2}$ it was required that the predicted series also describe a variation similar to the observed one, i.e. TSI ^{forc}(1983)<TSI ^{forc}(1993)<TSI ^{forc}(2003)>TSI ^{forc}(2013) in the case of TSID $_{U}$ and TSI ^{forc}(1983)>TSI ^{forc}(1993)>TSI ^{forc}(2003)>TSI ^{forc}(2013) in the case of TSI $_{PMOD}$.

Thus, the probability P_2 was estimated.

The probabilities of both outcomes (*a*) and (*b*) were determined using 10,000 trials and were considered as a measure of forecast quality. They are shown in Table 2 along with prediction errors STD_{pred}^{obs} . The dependence of the quality of nonlinear predictions on the standard deviations of the TSI reconstructions used is illustrated in Fig. 5.

TABLE 2

FIG. 5

4. CONCLUSIONS

The analysis based on nonlinear prediction showed the following.

Overall, the observed TSI values are better predicted using reconstructions with small amplitude of long-term variations. "Extreme" TSI reconstructions [Shapiro et al., 2011; Egorova et al., 2018] appear less realistic. Linear predictions made using a second-order autoregressive model led to similar results. The worst prediction was obtained using the Shapiro et al. [2011] reconstruction, which is consistent with the results of Judge et al. [2012], who concluded that the amplitudes of long-term TSI changes in this reconstruction were likely overestimated. Overall, the obtained results are consistent with the conclusions of Yeo et al. [2020], who concluded that TSI after the Maunder Minimum increased by no more than 2.0±0.7 W m $^{-2}$. It can be noted that an even lower limit for the increase after the Maunder Minimum - 1.25 W m $^{-2}$ - was obtained in the work of Lockwood and Ball [2020]. On the other hand, fairly accurate predictions were also obtained using the reconstruction from Bard et al. [2000], in which the TSI increase after the Maunder Minimum reached 2.5 W m $^{-2}$. Their quality was not worse than the quality of predictions obtained using MA reconstructions.

Most of the obtained predictions show a decreasing trend throughout all 40 years, which is consistent with the experimental PMOD series, as well as semi-empirical models SATIRE-S, NRLTSI2 and NRLTSI3 [Dudok de Wit et al., 2017; Lean et al., 2020].

On the one hand, the fact that MA reconstructions better predict the observed changes in TSI is not surprising. The results of total solar radiation measurements since 1978 indicate that long-term changes in its mean value are insignificant. Their amplitude is probably no more than 0.2 W m $^{-2}$ (see

Fig. 1 *b*) **,** so this value is not for nothing called the solar constant. This behavior better agrees with MA reconstructions, the amplitude of secular variations of which usually does not exceed 0.5–1.0 W m $^{-2}$. On the other hand, the possibility that TSI experienced more powerful fluctuations in the past with an amplitude of up to 2.5 W m $^{-2}$ cannot be completely excluded. The obtained results indicate that when conducting climate modeling, it is necessary to carefully justify the choice of TSI reconstructions with very low amplitude of long-term variations. For example, if the increase in TSI after the Maunder Minimum is indeed 2.5 W m $^{-2}$, which is observed not only in the Bard et al. [2000] series, but also in the shorter (five centuries) reconstruction by Penza et al. [2022], then the corresponding radiative forcing will reach 0.43 W m $^{-2}$. This can cause a rise in global temperature by 0.3°C. To clarify the question of what was the amplitude of secular changes in TSI in the past, further research is needed, including: (*a*) − obtaining new long-term reconstructions of TSI variations in the past and (*b*) − refining data on long-term variations of experimentally measured TSI. Further careful photometric monitoring of sun-like stars can also help solve this problem.

REFERENCES

1. *Bard E., Raisbeck G., Yiou F., Jouzel J* . Solar irradiance during the last 1200 years based on cosmogenic nuclides // Tellus B. V. 52. N 3. P. 985−992. 2000. https://doi.org/10.1034/j.1600-0889.2000.d01-7.x.
2. *Chatzistergos T., Krivova N.A., Yeo K.L.* Long-term changes in solar activity and irradiance // J. Atmos. Sol.-Terr. Phy. V. 252. ID 106150. 2023. https://doi.org/10.1016/j.jastp.2023.106150.
3. *Connolly R., Soon W., Connolly M . et al.* How much has the Sun influenced Northern Hemisphere temperature trends? An ongoing debate // Res. Astron. Astrophys. V. 21. N 6. ID 131. 2021. https://doi.org/10.1088/1674-4527/21/6/131.
4. *Delaygue G., Bard E* . An Antarctic view of Beryllium-10 and solar activity for the past millennium // Clim. Dynam. V. 36. N 11. P. 2201−2218. 2011. https://doi.org/10.1007/s00382-010-0795-1.
5. *Dewitte S., Cornelis J., Meftah M* . Centennial total solar irradiance variation // Remote Sensing . V. 14. N 5. ID 1072. https://doi.org/10.3390/rs14051072. 2022.
6. *Dudok de Wit T., Kopp G., Fröhlich C., Schöll M* . Methodology to create a new total solar irradiance record: making a composite out of multiple data records // Geophys. Res.

7. Lett. V. 44. N 3. P. 1196−1203. 2017. https://doi.org/10.1002/2016GL071866.
8. *Egorova T., Schmutz W., Rozanov E., Shapiro A.I., Usoskin I., Beer J., Tagirov R.V., Peter T.* Revised historical solar irradiance forcing // Astron. Astrophys. V. 615. ID A85. 2018. https://doi.org/10.1051/0004-6361/201731199.
9. *Farmer J.D., Sidorowich J* . Predicting chaotic time series // Phys. Rev. Lett. V. 59. N 8. P. 845−848. 1987. https://doi.org/10.1103/PhysRevLett.59.845.
10. *Gulev S.K., Thorne P.W., Ahn J . et al.* Changing state of the climate system / Climate Change 2021: The Physical Science Basis. Contribution of Working Group I to the Sixth Assessment Report of the Intergovernmental Panel on Climate Change. Eds. P. Masson-Delmotte, V. Zhai, A. Pirani et al. Cambridge, UK and New York, NY, USA: Cambridge University Press. P. 287–422. 2021. https://doi.org/10.1017/9781009157896.004.
11. IPCC. 2014 / Climate Change 2014: Synthesis Report. Contribution of Working Groups I. II and III to the Fifth Assessment Report of the Intergovernmental Panel on Climate Change (Core Writing Team). Eds. R.K. Pachauri, L.A. Meyer. Geneva, Switzerland: IPCC, 151 p. 2014.
12. IPCC. 2021- Summary for Policymakers / Climate Change 2021: The Physical Science Basis. Contribution of Working Group I to the Sixth Assessment Report of the Intergovernmental Panel on Climate Change. Eds. P. Masson-Delmotte, V. Zhai, A. Pirani et al. Cambridge, UK and New York, NY, USA: Cambridge University Press. P. 3−32. 2021. https://doi:10.1017/9781009157896.001.
13. *Judge P.G., Lockwood G.W., Radick R.R., Henry G.W., Shapiro A.I., Schmutz W., Lindsey C.* Confronting a solar irradiance reconstruction with solar and stellar data // Astron. Astrophys . V. 544. ID A88. 2012. https://doi.org/10.1051/0004-6361/201218903.
14. *Jungclaus J.H., Bard E., Baroni M. et al.* The PMIP4 contribution to CMIP6 – Part 3: The last millennium, scientific objective, and experimental design for the PMIP4 past1000 simulations // Geosci. Model Dev. V.10. N 11. P. 4005–4033. 2017. https://doi.org/10.5194/gmd-10-4005-2017.
15. *Kopp G.* Magnitudes and timescales of total solar irradiance variability // J. Space Weather Spac. V. 6. ID A30. 2016. https://doi.org/10.1051/swsc/2016025
16. *Lean J.* Evolution of the Sun's spectral irradiance Since the Maunder Minimum // Geophys. Res. Lett. V. 27. N 16. P. 2425-2428. 2000. https://doi.org/10.1029/2000GL000043.

17. *Lean J.L., Coddington O., Marchenko S.V . , Machol J., DeLand M.T., Kopp G.* Solar irradiance variability: Modeling the measurements // Earth and Space Science. V. 7. N 8. ID e2019EA000645. 2020. https://doi.org/10.1029/2019EA000645.
18. *Lockwood M., Ball W.T* . Placing limits on long-term variations in quiet-Sun irradiance and their contribution to total solar irradiance and solar radiative forcing of climate // P. Roy. Soc. A. -Mat. Phy. V. 476. N 2238. ID 20200077. 2020. https://doi.org/10.1098/rspa.2020.0077.
19. *Matthes K., Funke B., Anderson M . et al.* Solar Forcing for CMIP6 (v3.2) // Geosci. Model Dev. V. 10. N 6. P. 2247-2302. 2017. https://doi.org/10.5194/gmd-10-2247-2017.
20. *Montillet J.-P., Finsterle W., Kermarrec G., Sikonja R., Haberreiter M., Schmutz W., Dudok de Wit T.* Data fusion of total solar irradiance composite time series using 41 years of satellite measurements // J. Geophys. Res. - Atmos. V. 127. N 13. ID e2021JD036146. 2022. https://doi.org/10.1029/2021JD036146.
21. *Ogurtsov M* . Prediction of cycle 24 based on information about solar activity during the last 10000 years // Geomagn. Aeronomy. V. 49. N 3. P. 408-411. 2009. https://doi.org/10.1134/S0016793209030165.
22. *Ogurtsov M* . New paleoclimatic evidence of an extraordinary rise in temperature in the Northern Hemisphere in the last 3-4 decades // Geogr. Ann. A. V. 104. N 4. P. 288-297. 2022. https://doi.org/10.1080/04353676.2022.2136454.
23. *Penza V., Berrilli F., Bertello L . , Cantoresi M., Criscuoli S., Giobbi P.* Total solar irradiance during the last five centuries // Astrophys. J. V. 937. N 2. ID 84. 2022. https://doi.org/10.3847/1538-4357/ac8a4b.
24. *Roth R., Joos F* . A reconstruction of radiocarbon production and total solar irradiance from the Holocene ^{14}C and CO_2 records: Implications of data and model uncertainties // Clim. Past. V. 9. N 4. P. 1879−1909. 2013. https://doi.org/10.5194/cp-9-1879-2013.
25. *Sarp V., Kilcik A., Yurchyshyn V . , Rozelot J.P., Ozguc A.* Prediction of solar cycle 25: A non-linear approach // Mon. Not. R. Astron. Soc. V. 481. N 3. P. 2981−2985. 2018. https://doi.org/10.1093/mnras/sty2470.
26. *Shapiro A.I., Schmutz W., Rozanov E .*, *Schoell M., Haberreiter M., Shapiro A.V., Nyeki S.* A new approach to the long-term reconstruction of the solar irradiance leads to large historical solar forcing // Astron. Astrophys. V. 529. ID A67. 2011. https://doi.org/10.1051/0004-6361/201016173.

27. *Solanki S.K., Krivova N.A., Haigh J.D* . Solar irradiance variability and climate // Annu. Rev. Astron. Astr. V. 51. N. 1. P. 311−351. 2013. https://doi.org/10.1146/annurev-astro-082812-141007.
28. *Steinhilber F., Abreu J.A., Beer J. et al.* 9.400 years of cosmic radiation and solar activity from ice cores and tree rings // P. Natl. Acad. Sci. USA. V. 109. N 16. P. 5967−5971. 2012. https://doi.org/10.1073/pnas.1118965109.
29. *Sugihara G., May R.M.* Nonlinear forecasting as a way of distinguishing chaos from measurement error in time series // Nature. V. 344. N 6268. P. 734−741. 1990. https://doi.org/10.1038/344734a0.
30. *Sugihara G.* Nonlinear forecasting for the classification of natural time series // Phil. T. Roy. Soc. A. V. 348. N 1688. P. 477−495. 1994. https://doi.org/10.1098/rsta.1994.0106.
31. *Wu C.-J., Krivova N.A., Solanki S.K., Usoskin I.G* . Solar total and spectral irradiance reconstruction over the last 9000 year // Astron. Astrophys. V. 620. ID A120. 2018. https://doi.org/10.1051/0004-6361/201832956.
32. *Yeo K. L., Solanki S.K., Krivova N.A . , Rempel M., Anusha L.S., Shapiro A.I., Tagirov R.V., Witzke V.* The dimmest state of the Sun // Geophys. Res. Lett. V. 47. N 19. ID e2020GL090243. 2020. https://doi.org/10.1029/2020GL090243.

Table 1. Solar activity reconstructions used in this work

Source	TSI indicators used	Period covered	Temporal resolution (years)	STD ($W \times m^{-2}$)	ΔTSI (1680-end of 20 th century) ($W \times m^{-2}$)	Reconstruction type
Delaygue and Bard [2011]	^{10}Be in ice from South Pole and Dome Fuji	695−1982	6−15	0.22	0.9	MA
Roth and Joos [2013]	^{14}C in tree rings (IntCal09)	0 – 10000 BP	1	0.23	0.75	MA
Wu et al. [2018]	^{10}Be in ice from Greenland and	last 9000 years	10	0.29	1.0	MA

	Antarctica, ^{14}C in tree rings					
Steinhilber et al. [2012]	^{10}Be in ice from Greenland and Antarctica, ^{14}C in tree rings	9362 BCE – 1978	22	0.32	1.15	MA
Bard et al. [2000]	^{10}Be in ice from South Pole	843–1961	1−22	1.21	3.4	BA
Egorova et al. [2018] (PHI-MC17)	^{10}Be in ice from Greenland and Antarctica, ^{14}C in tree rings	6000 BCE –2015	1	1.31	4.9	BA
Shapiro et al. [2011]	^{10}Be in ice from Greenland and Antarctica, instrumental data	500 BCE – 2000	1	2.36	6.4	BA

Table 2. Quality assessment of nonlinear prediction of actually observed total solar irradiance, performed using seven paleoreconstructions of this value

Source	STD (W×m $^{-2}$)	TSID $_{C\ forecast}$			TSID $_{U\ forecast}$			TSI $_{PMOD\ forecast}$		
		STD_{pred}^{obs} (W×m $^{-2}$)	P_1	P_2	STD_{pred}^{obs} (W×m $^{-2}$)	P_1	P_2	STD_{pred}^{obs} (W×m $^{-2}$)	P_1	P_2
Delaygue and Bard [2011]	0.22	0.155	1.000	0.077	0.238	1.000	0.114	0.361	1.000	0.062
Roth and Joos [2013]	0.23	0.130	1.000	0.108	0.216	1.000	0.127	0.371	1.000	0.102
Wu et al. [2018]	0.29	0.140	1.000	0.086	0.349	1.000	0.083	0.250	1.000	0.061

Steinhilber et al. [2012]	0.32	0.392	0.976	0.088	0.409	0.973	0.114	0.181	1.000	0.046
Bard et al. [2000]	1.21	0.118	0.912	0.115	0.259	0.905	0.118	0.309	0.904	0.052
Egorova et al. [2018] (PHI-MC17)	1.37	1.277	0.431	0.033	1.291	0.412	0.0450	0.892	0.584	0.038
Shapiro et al. [2011]	2.38	2.428	0.101	0.013	2.487	0.097	0.007	2.341	0.120	0.004

FIGURE CAPTIONS

Fig. 1 . (*a*) – yearly averaged composite data series of instrumentally measured TSI. Black line with filled squares – uncorrected series $TSID_U$; gray line with filled squares – corrected series $TSID_C$; dashed line with empty squares – corrected series TSI_{PMOD}. (*b*) – decadal averaged data of instrumentally measured TSI. Black line with filled squares – $TSID_U$, gray line with filled squares – $TSID_C$, dashed line with empty squares – TSI_{PMOD}.

Fig. 2 . TSI reconstructions normalized to the experimentally measured $TSID_C$ series. (*a*) – Delaygue and Bard [2011]; (*b*) – Roth and Joos [2013]; C – Wu et al. [2018]; (*d*) – Steinhilber et al. [2012]; (*e*) – Bard et al. [2000]; (*f*) – Egorova et al. [2018], PHI-MC17; (*g*) – Shapiro et al. [2011].

Fig. 3 . (*a*) – Correlation coefficient between the actually observed and predicted values, calculated for the four solar reconstructions used in the work; (*b*) – prediction error for these four reconstructions. Calculations were carried out using reconstructions: Steinhilber et al. [2012] (thin black line with solid squares); Delaygue and Bard et al. [2011] (bold black line with empty circles); Roth and Joos [2013] (dashed black line with empty squares), Egorova et al. [2018] (dashed gray line with empty circles). Prediction errors were estimated using uncertainties in TSI reconstructions.

Fig. 4 . Actually observed $TSID_C$ value (gray line with solid circles) and its predictions (black lines with empty circles) made based on paleoreconstructions: (*a*) Wu et al. [2018]; (*b*) Steinhilber et al. [2012]; (*c*) Delaygue and Bard et al. [2011]; (*d*) Roth and Joos [2013]; (*e*) Bard et al. [2000];

(*f*) Shapiro et al. [2011]; (*g*) Egorova et al. [2018].

Fig. 5. Dependence of nonlinear prediction quality on STD for various paleoreconstructions. (*a*) – prediction error made for $TSID_C$; (*b*) – prediction probability P_2 made for $TSID_C$; (*c*) – prediction error made for $TSID_U$; (*d*) – prediction probability P_2 made for $TSID_U$; (*e*) – prediction error made for TSI_{PMOD}; (*f*) – prediction probability P_2 made for TSI_{PMOD}.

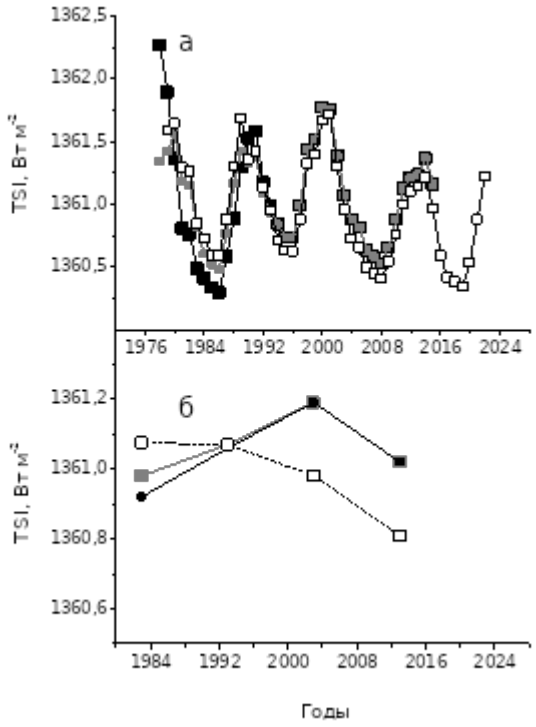

Fig. 1.

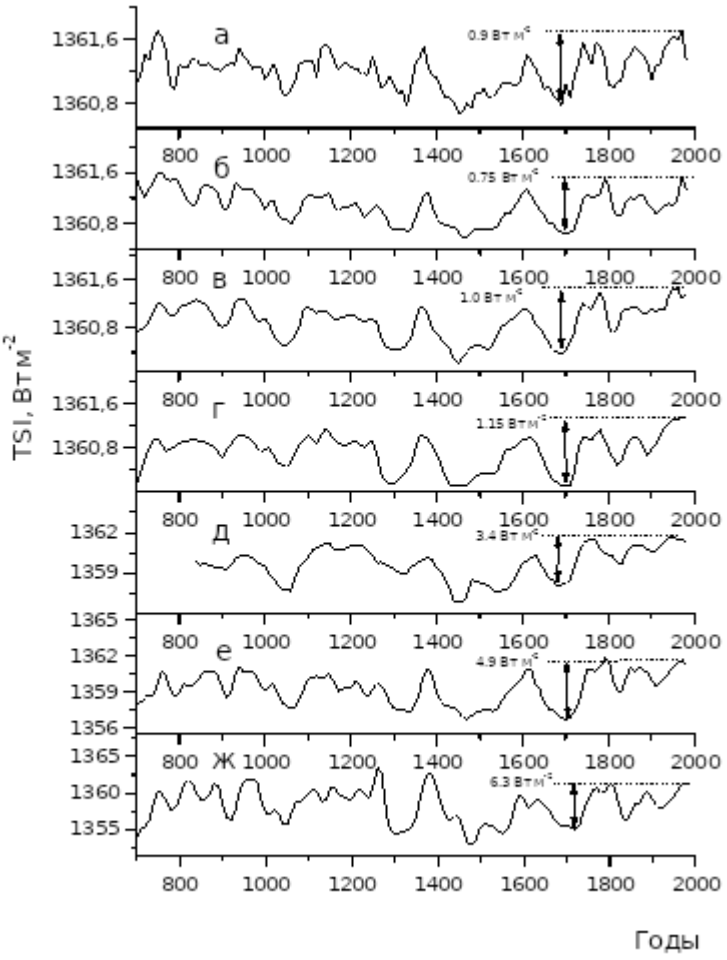
а
б
в
г
д
е
Ж
0.9 Вт м-2
0.75 Вт м-2
1.0 Вт м-2
1.15 Вт м-2
3.4 Вт м-2
4.9 Вт м-2
6.3 Вт м-2
TSI, Вт м-2
Годы

Fig. 2.

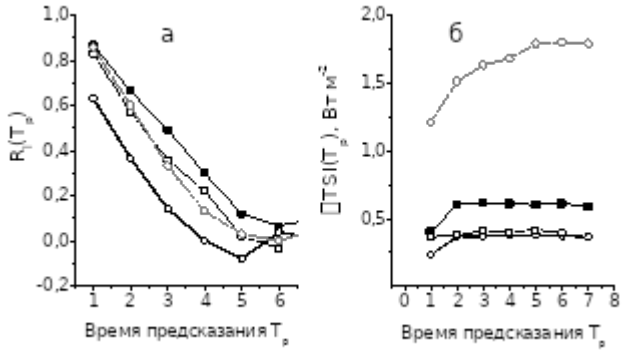
а
б
Время предсказания Tp
Время предсказания Tp

Fig. 3.

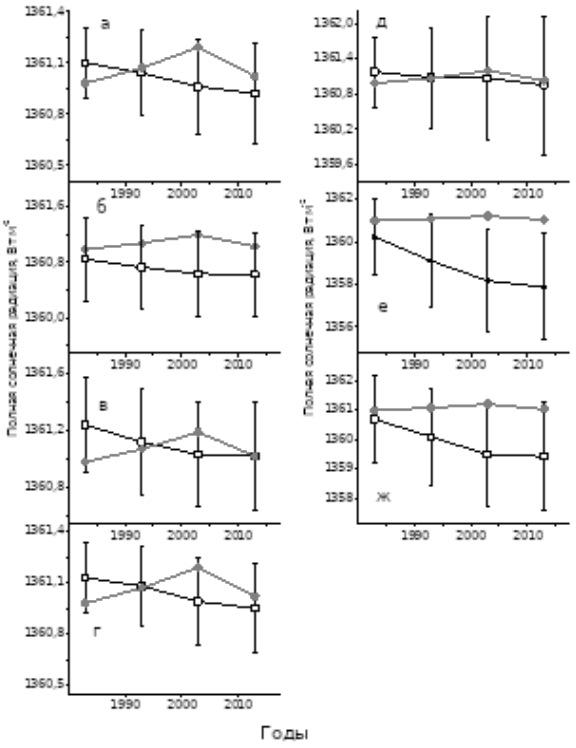
Полная солнечная радиация, Вт·м⁻²
Годы
а
б
в
г
д
е
ж
1990
2000
2010

Fig. 4.

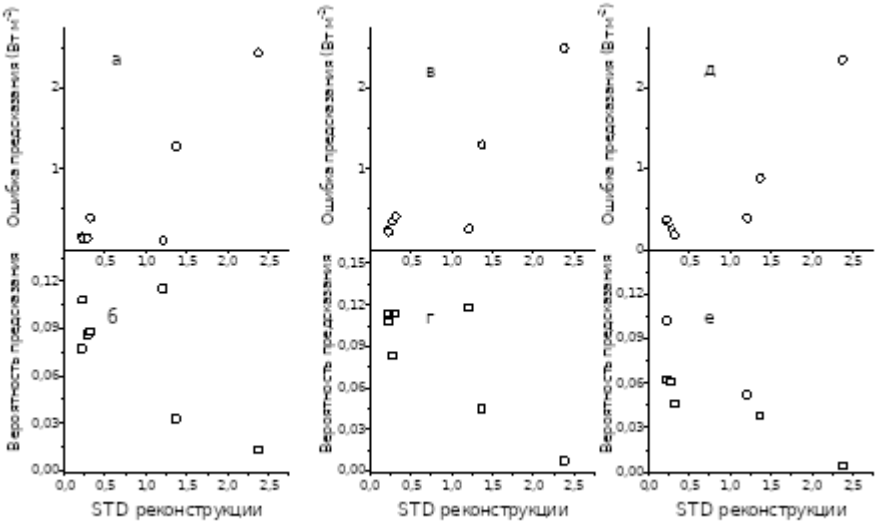
Ошибка предсказания (Вт·м⁻²)
Вероятность предсказания
STD реконструкции
а
б
в
г
д
е

Fig. 5.